ARTICLE
Journal of Cellular Biochemistry 113:1623–1634 (2012)

Journal of Cellular Biochemistry

Oxidative-Mechanical Stress Signals Stem Cell Niche Mediated Lrp5 Osteogenesis in eNOS$^{-/-}$ Null Mice

Nalini M. Rajamannan*

Division of Cardiology, Northwestern University Feinberg School of Medicine, Chicago, Illinois

ABSTRACT

Calcific aortic valve disease (CAVD) is the most common indication for valve surgery in the USA. This study hypothesizes that CAVD develops secondary to Wnt3a/Lrp5 activation via oxidative-mechanical stress in eNOS null mice. eNOS$^{-/-}$ mice were tested with experimental diets including a control (n = 20), cholesterol (n = 20), cholesterol + Atorvastatin (n = 20). After 23 weeks the mice were tested for the development of aortic stenosis by Echo, Histology, MicroCT, and RTPCR for bone markers. In vitro studies measured Wnt3a secretion from aortic valve endothelial cells and confirmed oxidative stress via eNOS activity. Anion exchange chromatography was performed to isolate the mitogenic protein. Myofibroblast cells were tested to induce bone formation. Cholesterol treated eNOS mice develop severe stenosis with an increase in Wnt3a, Lrp5, Runx2 (threefold increase ($P < 0.0001$) in the bicuspid versus tricuspid aortic valves. Secretion of Wnt3a from aortic valve endothelium in the presence of abnormal oxidative stress was correlated with diminished eNOS enzymatic activity and tissue nitrite levels. Initial characterization of the architecture for a stem cell nice was determined by protein isolation using anion-exchange chromatography and cell proliferation via thymidine incorporation. Osteoblastogenesis in the myofibroblast cell occurred via Lrp5 receptor upregulation in the presence of osteogenic media. Targeting the Wnt3a/Lrp5 pathway in valve calcification and activation of osteogenesis is via an oxidative-mechanical stress in CAVD. These findings provide a foundation for treating this disease process by targeting the cross talk mechanism in a resident stem cell niche. J. Cell. Biochem. 113: 1623–1634, 2012.

KEY WORDS: VALVULAR HEART DISEASE; LIPIDS; ENOS; LRP5

Calcific aortic valve disease (CAVD) is the most common indication for surgical valve replacement. For years this disease was thought to be a passive degenerative phenomenon. However, the cellular mechanisms involving this disease process are emerging. There are two forms of CAVD, tricuspid aortic valve disease and bicuspid aortic valve (BAV) disease. BAV is the most common congenital cardiac anomaly, having a prevalence of 0.9–1.37% in the general population [Roberts and Ko, 2005]. BAV disease occurs more frequently in patients who are undergoing surgical valve replacement. Understanding of the cellular mechanisms of the mechanisms of aortic valve lesions will present further understanding towards slowing disease progression. Currently, there are three fundamental cellular mechanisms defined in the development of aortic valve disease: (1) oxidative stress via traditional cardiovascular risk factors [Rajamannan et al., 2002ab, 2003a, 2005ab; Drolet et al., 2003; Makkena et al., 2005; Weiss et al., 2006; Aikawa et al., 2007], (2) cellular proliferation [Rajamannan et al., 2001b], and (3) osteoblastogenesis in the end stage disease process [Mohler et al., 2001; Rajamannan et al., 2003b].

Previously, the Wnt/Lrp5 signaling pathway has been identified as a signaling mechanism for cardiovascular calcification [Shao et al., 2005; Rajamannan et al., 2005a; Caira et al., 2006]. This study tests the hypothesis [Rajamannan, 2011a] that the cellular architecture resident in the valve is necessary to mediate the disease phenotype via two co-regulatory mechanisms: first an endothelial–mesenchymal cross-talk oxidative stress signal, and second a lipid-mechanical force signal to regulate the Lrp5 receptor upregulation in the aortic valve myofibroblast cell. The study will examine these two mechanisms by: (1) an in vivo mouse model, (2) characterize the secretion of a Wnt3a from the aortic valve endothelium in the presence of lipids and lipid lowering medication, (3) measures osteogenic activity in the myofibroblast cell, and (4) isolates the mitogenic activity to prove the cell–cell signaling cross talk mechanism.

*Correspondence to: Nalini M. Rajamannan, MD, Northwestern University, 303 E. Chicago, Suite 12-717, Chicago, IL 60611. E-mail: nrajamannan@gmail.com

Received 6 December 2011; Accepted 7 December 2011 • DOI 10.1002/jcb.24031 • © 2011 Wiley Periodicals, Inc.
Published online 22 December 2011 in Wiley Online Library (wileyonlinelibrary.com).

MATERIALS AND METHODS

eNOS$^{-/-}$ MOUSE MODEL OF BICUSPID VERSUS TRICUSPID AORTIC VALVE DISEASE

eNOS$^{-/-}$ mice (B6.129P2-Nos3t^{m1Unc}/J) were purchased from Jackson Laboratories (Bar Harbor, Maine). Mice age 6–8 weeks were purchased from Jackson Laboratories. These mice assigned to a control (N = 60), a 0.2% cholesterol (w/w) diet (Harlan Teklad 88137), (N = 60), and a 0.2% cholesterol (w/w) diet (Harlan Teklad 88137) plus atorvastatin 0.1% (v/v) in drinking water (N = 60). All animals were fed ad libitum for 23 weeks. Control mice were fed a standard diet. Following this 23-week period, the mice were anesthetized using inhalation isoflurane for the echocardiography studies and then euthanasia with inhalation CO_2. All experiments were performed in an animal facility accredited by the Association for Assessment and Accreditation of Laboratory Animal Care, Inc. (ACUC-A3283-01, 1-08-382). Immediately after dissection from the heart, and fixed in 10% buffered formalin for 48 h, transferred to 70% Ethanol and then embedded in paraffin. Valves were also snap frozen in liquid nitrogen and stored in −80°C freezer for gene expression experiments. Paraffin embedded sections (6 μm) were cut and prepped for histopathologic exam.

VISUAL SONICS MOUSE ECHOCARDIOGRAPHY

Comprehensive transthoracic echocardiograms were performed using the Visual Sonics Echocardiographic Machine (Toronto, CA). Standard doppler measurements of left ventricular outflow tract and aortic valve from multiple windows to obtain the maximum velocity were recorded and the mean gradient, the peak velocity and aortic valve area were measured and calculated as previously described [Rajamannan, 2011c]. Screening for the bicuspid phenotype found a similar prevalence to previously published data [Lee et al., 2000]. Table I demonstrates the echocardiographic features of the two different mouse phenotypes.

MICRO-CT

After fixing in formalin, the valves were examined using a Scanco MicroCT-40 system operated at 45 kV. Sampling was with ~8 μm voxels (volume elements) and maximum sensitivity (1,000 projections, 2,048 samples and 0.3 s/projection integration [Rajamannan et al., 2003b]) N = 10 valves total were tested [Rajamannan et al., 2003b, 2005a].

BONE TAG INJECTION AND Li-Cor MOLECULAR IMAGING

To measure rates of bone turnover we inject the eNOS$^{-/-}$ mice with Bone tag 48 h prior to sacrifice. The Bone Tag incorporates in areas of active bone turnover [Westerlind et al., 1997; Kovar et al., 2007]. The system measures near infrared fluorochromes to assess newly forming bone in tissues. Important criteria for effective optical imaging fluorochromes include: excitation and emission maxima in the near infrared range (NIR) between 700 and 900 nm; high quantum yield; chemical and optical stability; and suitable pharmacological properties including aqueous solubility, low nonspecific binding, rapid clearance of the free dye and low toxicity [Kovar et al., 2007]. We injected the eNOS with the 3 different diets with the IRDye 800 CW dye (Bone Tag Probe-conjugated tetracycline derivative), and measured the optimal imaging of the mice testing first the entire mouse, and then the individual organs. We found that the 48 h injections provided the

TABLE I. Quantification of the RTPCR, LiCor Bone Probe Measurements in the Valves and Femurs From the eNOS$^{-/-}$ Bicuspid Mice

	Control	Cholesterol	Cholesterol + atorva statin
Echocardiographic data			
Bicuspid			
EF%	64.64 ± 10	60.00 ± 10	53.00 ± 8
Peak jet velocity	1.38 ± 0.25	3.93 ± 0.37*	1.63 ± 0.75**
Tricusoid			
EF%	67.11 ± 9	59.54 ± 8	56.31 ± 9
Peak jet velocity	1.07 ± 0.23	1.57 ± 0.17	1.51 ± 0.21
Quantification of gene expression: bicuspid aortic valve			
Runx2	0.456 ± 0.0443	0.562 ± 0.0573	0.467 ± 0.0269
Cyclin	0.575 ± 0.103	1.057 ± 0.714	0.566 ± 0.370
Osteopontin	0.350 ± 0.204	0.590 ± 0.218	0.398 ± 0.242
Lrp5	0.729 ± 0.271	1.057 ± 0.112*	0.788 ± 0.262**
Wnt3a	0.399 ± 0.0632	0.698 ± 0.134*	0.387 ± 0.156**
Quantification of gene expression: tricuspid aortic valve			
Runx2	0.108 ± 0.0482	0.196 ± 0.102	0.081 ± 0.0114
Cyclin	0.114 ± 0.0487	0.331 ± 0.252	0.104 ± 0.0122
Osteopontin	0.212 ± 0.0654	0.413 ± 0.288	0.123 ± 0.0225
Lrp5	0.839 ± 0.375	1.215 ± 0.168	1.15 ± 0.329
Wnt3a	0.208 ± 0.0189	0.229 ± 0.0193**	0.261 ± 0.0541**
Quantification of gene expression: femurs			
Runx2	0.118 ± 0.00952	0.160 ± 0.0305*	0.116 ± 0.0196**
Cyclin	0.752 ± 0.424	0.763 ± 0.436	0.529 ± 0.245
Osteopontin	0.406 ± 0.0889	0.524 ± 0.0391*	0.455 ± 0.100
Lrp5	0.241 ± 0.0895	0.213 ± 0.0479*	0.334 ± 0.100**
Wnt3a	0.196 ± 0.0126	0.256 ± 0.0222*	0.180 ± 0.0539**
Quantification Li-Cor molecular imaging			
Hearts	177 ± 0.03	471 ± 0.08*	281 ± 0.02**
Femurs	3,120 ± 0.02	4,265 ± 0.02*	3,105 ± 0.09**

Quantification of the echocardiographic results of the tricuspid versus bicuspid aortic valves in the eNOS null mice.
*$P<0.05$ control versus cholesterol.
**$P<0.05$ cholesterol versus cholesterol + atorvastatin.

most specific data allowing for the proper wash out period for the dye. (24, 48, and 72 h were tested for the protocol of N = 60 mice.)

IN VITRO MODEL VALVULAR FIBROBLAST CELLS AND AORTIC VALVE ENDOTHELIAL PORCINE CELLS

Valvular fibroblast cells and endothelial cells are obtained from mature Yorkshire pigs and isolated from the cardiac aortic valves by collagenase digestion [Rajamannan et al., 2001a]. Cells will be cultured in medium 199 with 10% (v/v) heat-inactivated fetal bovine serum at 37°C in a humidified atmosphere of 5% CO_2 in air. Cells are utilized between the 3rd and 10th passage. Conditioned media from aortic valve endothelial cells was produced by treating the cells for 24 h with low density lipoprotein (LDL) (10 ng/ml) (Intracell, Fredrick, MD), LDL + atorv (10^{-6}M), and atorv (10^{-6}M) alone. The conditioned media was then tested directly on the aortic valve myofibroblast cells for 18 h in quadruplicate wells and pulsed with 1 μCi/well of tritiated thymidine for the final 4 h of the incubation. Dose response experiments for LDL and atorvastatin were performed, and the data shown is the peak dose for these effectors [Rajamannan et al., 2005a]. Newly synthesized DNA was identified by incorporation of radioactivity into acid-precipitated cellular material [Rajamannan et al., 2001a]. Platelet-derived growth factor (PDGF) will serve as a positive control for proliferation, and incubation in serum-free medium alone as a negative control (N = 12 replicates were performed). Western blot analysis was also performed on the different treatment groups as outlined in the Western blot methods (N = 3 replicates).

THYMIDINE ASSAY

Cardiac valve fibroblast cells will be grown to confluence in 24-well plates and then growth-arrested by incubation in serum-free medium for 24 h. The factors to be tested are then incubated with cells for 18 h in quadruplicate wells and pulsed with 1 μCi/well of tritiated thymidine for the final 4 h of the incubation. Newly synthesized DNA will be identified by incorporation of radioactivity into acid-precipitated cellular material [Rajamannan et al., 2001a].

WESTERN BLOT

Western blot analysis was performed as previously described [Rajamannan et al., 2005a]. [Anti-Dkk1 (Chemicon, International, Temecula, CA), Wnt3a (R and D systems, Minneapolis), and anti-caveolin-1 and anti-Enos (Abcam, Cambridge, MA)]. We performed (N = 3) replicates on each Western blot experiment, and show a representative experiment for the data.

SEMI-QUANTITATIVE REVERSE TRANSCRIPTASE POLYMERASE CHAIN REACTION

Immediately after dissection from the heart, the leaflets from each aortic valve and the femurs were frozen in liquid nitrogen for RNA extraction. Messenger RNA was isolated using MicroFast Track (Invitrogen), and 4 μg of RNA was used for semi-quantitative reverse transcriptase polymerase chain reaction (RTPCR) analysis. RTPCR was performed to determine expression levels of Wnt3a (326 bp), Lrp5 (667 bp), Runx2 (289 bp), osteopontin (102 bp), cyclin (151 bp), and GAPDH (451 bp) as previously described [Caira et al., 2006].

IMMUNOGOLD ELECTRON MICROSCOPY

The valve leaflets were fixed in 4% formaldehyde plus 0.2% glutaraldehyde in phosphate buffer overnight, rinsed in phosphate buffer, partially dehydrated to 80% ethanol and embedded in LR White resin. Thin sections (~0.1 μm) were mounted on nickel grids and labeled with an antibody to eNOS and caveolin1 (Abcam). Prior to labeling, the sections were treated with phosphate buffered saline with 0.05% Tween 20 (PBS-T), 1% (w/v) glycine, and 2% (w/v) normal goat serum for 15 min. Sections were then incubated in undiluted primary antibody for 2 h at room temperature. After rinsing extensively in PBS-T, the sections were incubated for 60 min in goat anti-mouse antibody conjugated to 10 nm gold diluted 1:50 in PBS-T. Grids were rinsed in PBS-T, rinsed in water, and dried. Sections were examined after staining with uranyl acetate and lead citrate.

ANIONIC MITOGEN ISOLATION

Cardiac valve endothelial cells and myofibroblast cells were isolated as previously described [Rajamannan et al., 2005a]. The endothelial cells were cultured on microcarrier beads to increase the surface area so as to increase the concentration of the transformed activity in the conditioned media [Rajamannan et al., 1988]. The conditioned media from these cells were chromatographed on diethylaminoethyl-dextran (DEAE–Sephadex, Sigma) as described in the preliminary results. Briefly, the resin was swollen and equilibrated with 0.015 M HEPES, pH 7.40. The conditioned media was dialyzed into the same buffer, 1.5 ml applied to a 0.5 cm × 1.0 cm DEAE–Sephadex column, and allowed to bind as a slurry at 4°C. The activity is eluted with a 15 ml gradient of 0–0.5 M NaCl, both in 0.015 M HEPES at pH 7.40. Fractions of 1 ml in size are collected and equilibrated with serum-free medium by a combination of dialysis at 4°C (two dialysate changes over 3 h) and desalted over Bio-gel P-6DG 0.8 ml columns (Biorad, Richmond, CA). The fractions were then added to the myofibroblast media and the affects on cell proliferation by the thymidine mitogen assay. Gel filtration was used with a Sephadex G-100 (Sigma) to further purify the activity.

ADENOVIRAL VECTORS AND VIRAL DELIVERY

Replication-incompetent serotype 5 adenoviral vectors, driven by the cytomegalovirus immediate-early promoter, were generated, propagated, and purified as previously described [Chen et al., 1997]. Viral titers were determined by plaque assay. Briefly, HEK-293 cells were plated on 60-mm tissue culture plates and allowed to become confluent. Dilutions (10^{-9}–10^{-11} M) of the virus were incubated with the cells for 1 h. The virus was then aspirated, and the cells were overlayered with 1% agarose in DMEM and 2% fetal bovine serum (FBS). Overlayering was repeated every 4–5 days to maintain the cultures. Viral plaques were counted every other day starting with day 7 after infection until plaque numbers stopped increasing. The vectors used in these studies encoded a cDNA sequence for bovine eNOS (AdCMVeNOS) or, alternatively, *Escherichia coli* β-gal reporter gene (AdCMVLacZ) in place of the deleted E1 region of the virus. After 24 h in culture, cells were washed with PBS and transduced with PBS and 0.5% albumin containing 100 multiplicity of infection of AdCMVLacZ or AdCMVeNOS for 1 h. The vector solution was then aspirated, cells were washed with PBS, and

complete culture medium was replaced. At 24 h after transduction, cells were prepared for thymidine cell proliferation assays.

NOS ACTIVITY ASSAY

The conversion of L-[^{3}H]arginine to L-[^{3}H]citrulline was used to determine NOS activity. Briefly, aortic valve endothelial cells were homogenized in a lysis buffer identical to that described for Western blotting. Samples were incubated with a buffer containing 1 mM NADPH, 3 μM tetrahydrobiopterin, 100 nM calmodulin, 2.5 mM $CaCl_2$, 50 mM L-valine, 10 μM L-arginine, and L-[^{3}H]arginine (0.2 μCi) at 37°C. To determine NOS activity, duplicate samples were incubated for 20 min in the presence and absence of 1 mM N^G-nitro-L-arginine methyl ester (L-NAME) or vehicle [Shah et al., 1997]. The reaction was terminated by the addition of 1 ml of cold stop buffer (20 mM HEPES, 2 mM EDTA, and 2 mM EGTA, pH 5.5), and the reaction mix was applied to a Dowex AG 50WX-8 resin column. Radiolabeled counts per minute of L-citrulline generation were measured and used to determine L-NAME-inhibited NOS activity.

MEASUREMENT OF NO PRODUCTION

After 24 h in culture, aortic valve endothelial cells were transduced treated with oxidized LDL with and without Atorvastatin. The day after transduction, eNOS-derived NO was stimulated by incubating cells in DMEM with 1 mM L-arginine and 10 μM of the eNOS agonist A-23187 or an equal volume of vehicle in place of A-23187. After 1 h, the medium was collected and analyzed for the stable NO byproduct, nitrite, using NO-specific chemiluminescence (Seivers NOA). Cells were then lysed for protein measurement using the Lowry assay. NO-specific chemiluminescence was performed [Shah et al., 1999]. A standard curve was generated using known nitrite standards. Samples were examined in duplicate, and nitrite readings were normalized for cellular protein.

MINERALIZATION ASSAY

Porcine valvular myofibroblast cells were grown for extended periods (42 days) in Osteogenic Media (Stem Cell Technologies, Vancouver, CA) to induce morphological changes with subsequent formation of bone-like nodules. Gene expression, and microCT were measured to determine Cbfa1 and Lrp5 gene expression. Matrix was detected using the Alcian Blue (21 days) and Alizarin red (42 days) stains as previously described [Caira et al., 2006]. The culture plates with the myofibroblasts at different treatments/stages will be fixed in neutral buffered formalin at 4°C overnight. Osteogenic media is necessary to induce osteoblastic differentiation in undifferentiated/immature osteoblast precursors and vascular smooth muscle cells [Stringa et al., 1995; Tintut et al., 2003; Kirton et al., 2007].

STATISTICS

Data presented for each diseased valve as an average of the percent of the internal control. The internal control was GAPDH for the PCR and Actin for the Western blot. One-way ANOVA was used to examine if there are differences in normalized gene and protein expression among diseased valves and the control valves. Significance of the test statistics is set at 0.05 level.

RESULTS

IN VIVO MOUSE MODEL OF CALCIFIC AORTIC VALVE DISEASE

To understand if eNOS$^{-/-}$ mice with the BAV phenotype, develops accelerated stenosis earlier than tricuspid aortic valves via the Lrp5 pathway activation, eNOS$^{-/-}$ mice were given a cholesterol diet versus cholesterol and atorvastatin. The Visual Sonics mouse echocardiography machine was used to screen for the BAV phenotype. Echocardiography hemodynamics was also performed to determine the timing of stenosis in bicuspid versus tricuspid aortic valves eNOS$^{-/-}$ mice on different diets. Figure 1 demonstrates the characterization of the eNOS phenotype as defined by histology, and echocardiography. In Figure 1, Panel A is the histology for BAV, Figure 1, Panel B is the microCT for the eNOS$^{-/-}$ mice hearts on the different diets. The bicuspid valves developed tiny areas of mineralization as indicated by the arrows in the hypercholesterolemic group and less with the cholesterol + Atorvastatin.

Figure 2, demonstrates the characterization of the eNOS phenotype as defined by Li-Cor near infrared imaging and RTPCR of the BAVs and the femurs of the eNOS null mice on the different diets. In Figure 2, Panel A is the infrared imaging of the whole mouse 48 h after injection with the bone tag. Imaging of the whole mouse demonstrated the highest concentration of the Bone Tag in the cholesterol diet mouse with less in the Atorvastatin and minimal in the control mice as shown by the green fluorescence. The red area in the image in the control mouse GI tract is the chlorophyll in the chow diet, which is part of the background that appears red with the NIR imaging. The Bone Tag (Green dye) shows up in the bones of the mice and any other areas of the mouse that is undergoing incorporation of the bone tag. Since the ribs and sternum, block the heart and therefore, do not allow for optimal in vivo imaging of the hearts. Individual organs were dissected including the hearts and femurs from the mice to image the tissues ex vivo.

The hearts in Figure 2, Panel B1, injected with the bone tag are in the top row. The control (Carboxylate) probe injected hearts are in the bottom row. The Pearl Imager then quantifies the amount of Bone Tag uptake into areas of active osteogenesis. The cholesterol hearts increased in the amount of bone tag uptake as compared to the control and Atorvastatin. The P values for the difference between the control versus cholesterol $P < 0.000161^{*}$ and the difference between the cholesterol and cholesterol + Atorv is $P < 0.01^{**}$. The femurs in Figure 2, Panel C1, injected with the bone tag are in the top row. The control probe injected femurs are in the bottom row. The cholesterol femurs demonstrate increase in active bone formation as compared to the control and the atorvastatin. The P values for the difference between the control versus cholesterol <0.08 and the difference between the cholesterol and cholesterol + Atorv is $<0.05^{**}$. Table I demonstrates the quantification data for the NIR imaging detection of the Bone Tag Fluorochrome and the echocardiographic data demonstrating that the BAV progresses to a more a severe stenosis than the tricuspid aortic valve from the eNOS$^{-/-}$ mice on the cholesterol diets. The Atorvastatin attenuates the stenosis present in the BAVs.

Figure 2, Panel B2 and C2, is the semi-quantitative RTPCR from the BAV and femurs, respectively. In the BAV as shown in Figure 2, Panel B2 and Table I, there was no change in the TAV obtained from

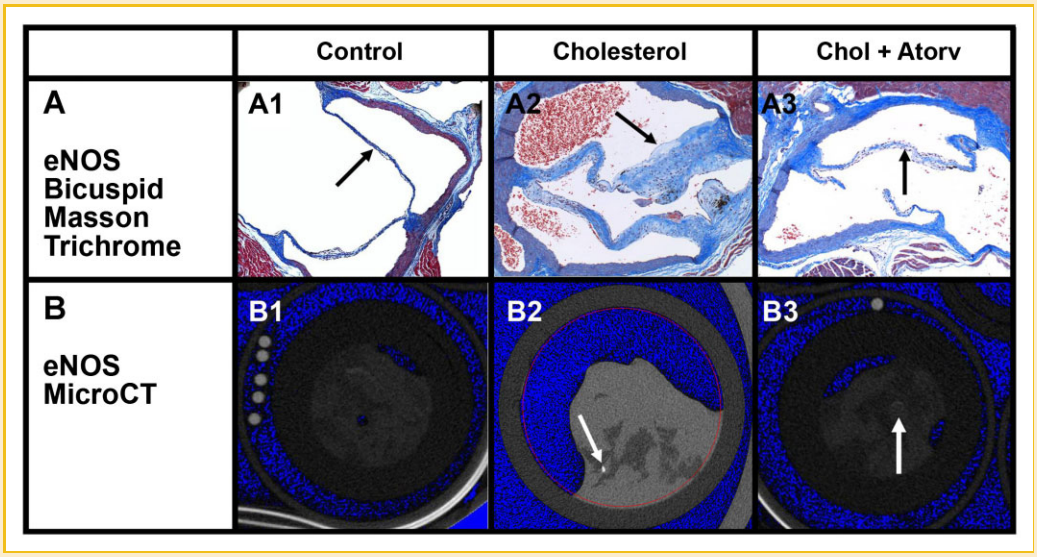

Fig. 1. Histology of the aortic valves from the eNOS$^{-/-}$ bicuspid mice. Panel (A): Masson Trichrome Stain of the eNOS$^{-/-}$ aortic valves on the control panel (A1), cholesterol panel (A2), and the cholesterol + atorvastatin diets panel (A3). Panel (B): MicroCT of the of eNOS$^{-/-}$ aortic valves on the control panel (B1), cholesterol panel (B2) and the cholesterol + atorvastatin diets panel (B3).

the eNOS$^{-/-}$ null mice from the different diets in terms of histology, RTCPR gene expression, and echocardiographic data. The gene expression for the femurs as shown in Figure 2, Panel C2, and Table I, demonstrated that Runx2, Lrp5, and Wnt3a increased in the cholesterol group and attenuation with atorvastatin. Quantification of the results are shown in Table I, with the P-value <0.05 considered significant.

IN VITRO MODEL OF ENDOTHELIAL–MYOFIBROBLAST CELL–CELL SIGNALING

Isolation of anionic mitogenic activity. Figure 3 demonstrates the isolation and characterization of the mitogenic protein from the conditioned media microenvironment. Endothelial cells were cultured as shown in Figure 3, Panel A, which is a light microscopy photograph of aortic valve endothelial cells isolated from the aortic surface of the aortic valve. The media was obtained from the endothelial cells and then transferred directly to the myofibroblast cell to determine effects on cell proliferation. The results of the mitogen assays for fractions eluting from a DEAE–Sephadex column are shown in Figure 3, Panel B. It can be seen that the mitogenic activity appeared as a single peak eluting at approximately 0.25 M NaCl. The material eluting from DEAE–Sephadex was then applied to Sephadex G-100; the results of mitogen assays on fractions eluting from such a gel filtration column are shown in Figure 3, Panel C. It can be seen that under these native, nondenaturing conditions the bulk of the mitogenic activity eluted as a peak corresponding to standard proteins of 30–40,000 molecular weight. This material lost all activity when heated to 100°C for 5 min; disulfide bond reduction with dithiothreitol also abolished all mitogenic activity; and treatment with trypsin destroyed all activity, implicating a protein structure. This data demonstrates the importance of the first corollary for defining a tissue stem cell niche: the physical architecture necessary for the signaling mechanisms. The endothelial lining cell along the aortic surface of the aortic valve signals to the myofibroblast cells that are resident below the endothelial cells to activate the disease process.

OXIDATIVE STRESS: THE ROLE OF ENDOTHELIAL NITRIC OXIDE SYNTHASE IN AORTIC VALVE ENDOTHELIAL CELLS

The second corollary for identifying a stem cell niche is to define the gradient responsible for the proliferation to differentiation process. To answer this question of the role of oxidative stress and nitric oxide in the aortic valve, in vitro experiments were performed to determine eNOS enzymatic and protein regulation in the presence of lipids and attenuation with Atorvastatin to confirm the importance of eNOS enzymatic function in vitro. Figure 4 demonstrates the eNOS regulation in the endothelial cells in the presence of lipids with and without Atorvastatin. A number of standard nitric oxide assays were performed to measure eNOS functional activity. Figure 4, Panel A1, tests for eNOS enzymatic activity in the aortic valve endothelial cells (AVEC) in the presence of LDL with and without Atorvastatin. eNOS enzymatic activity was decreased in the presence of lipids and Atorvastatin improved functional enzyme activity. Figure 4, Panel A2, shows results for tissue nitrites measured in the endothelial cells providing indirect evidence for the enzyme activity. There was an increase is nitrites with lipid treatments and attenuation with Atorvastatin. This increase in nitrite levels correlates with a decrease in the functional activity of the eNOS enzyme in the aortic valve endothelium.

The proof of principle experiment to test the importance of eNOS enzymatic activity is an overexpression experiment to determine if eNOS is able to inhibit cell proliferation, an early cellular event in the development of aortic stenosis [Rajamannan et al., 2001b]. Experiments were performed to overexpress eNOS to determine if

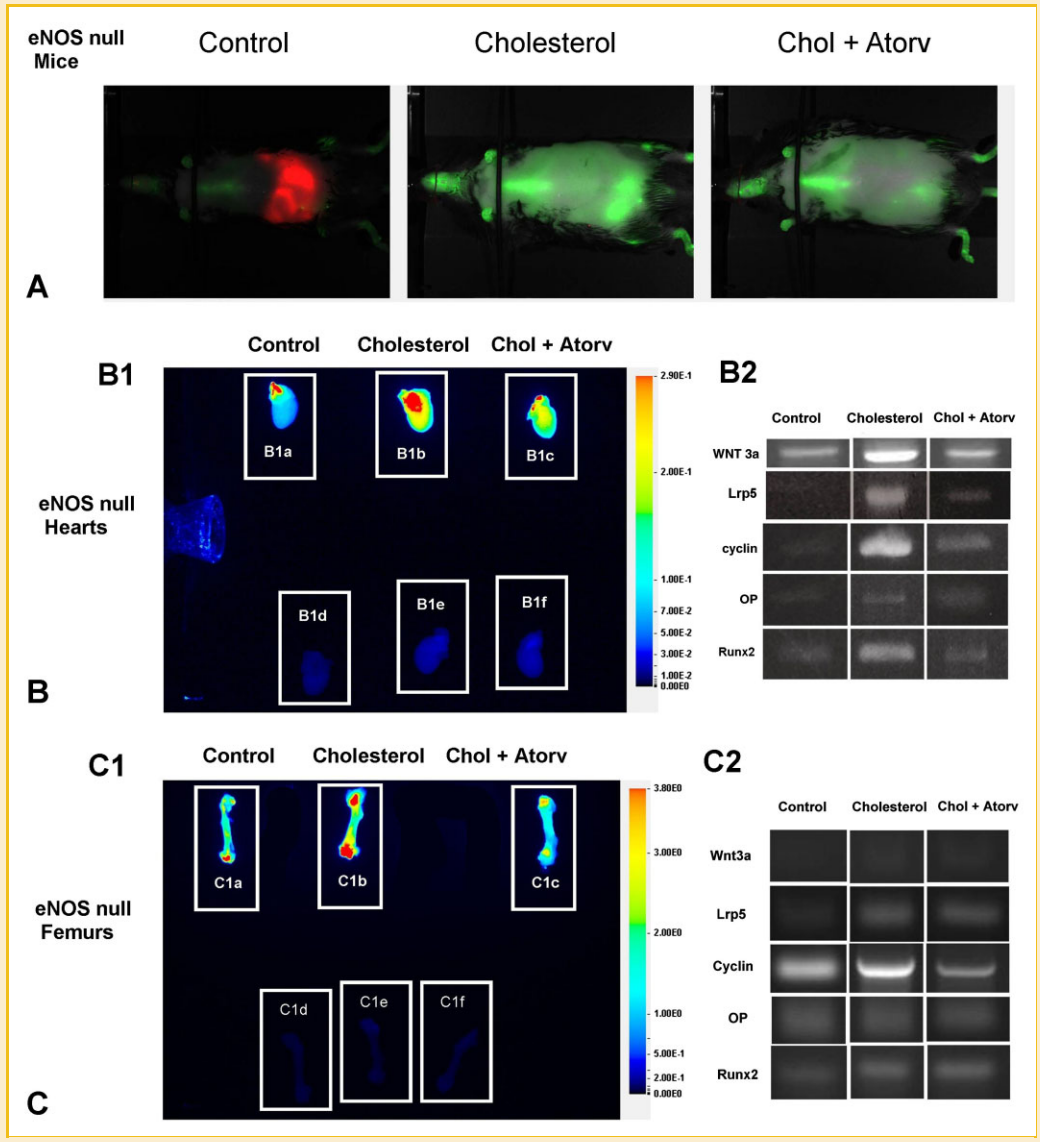

Fig. 2. Characterization of the bicuspid aortic valve and femurs in eNOS null mice by licor infrared imaging. Left column, control diet; middle column, cholesterol diet; right column, cholesterol diet plus atorvastatin. In each panel, the aortic valve leaflet is in the center (All frames 20× magnification). $^{*}P < 0.001$ for control compared to cholesterol, $^{**}P < 0.001$ for cholesterol compared to cholesterol + atorvastatin. Panel (A) infrared imaging of the entire mouse on each diet. Panel (B1) infrared imaging of the bicuspid hearts. Panel (B2) RTPCR on the aortic valves for Wnt3a, Lrp5, Cyclin1, OP, Runx2, GAPDH. Panel (C1) infrared imaging of the bicuspid hearts. Panel (C2) RTPCR on the femurs for Wnt3a, Lrp5, Cyclin1, OP, Runx2, GAPDH.

eNOS overexpression in the aortic valve endothelial cells would regulate cell proliferation. The in vitro myofibroblast cells were directly transduced with an eNOS adenoviral gene construct. Thymidine incorporation was measured to test if overexpressing eNOS can inhibit cellular proliferation. Figure 4, Panel A3, eNOS overexpression inhibits the cell proliferation in the oxidized LDL treated cells induced as compared to the LacZ control treated cells.

Experiments were performed to localize the expression of Caveolin1 and eNOS in the aortic valve endothelial cell caveolae. Figure 4, Panel B1, demonstrates that Caveolin-1 is upregulated in the lipid treated cells and decreases with atorvastatin treatment with no change in the eNOS protein expression as shown by Western blot. Figure 4, Panel B2, demonstrates the ultrastructural evidence by immunogold labeling for eNOS and Caveolin-1 present in the aortic valve endothelial cells in caveolae, similar to previously reported data [Rajamannan et al., 2002a, 2005b]. This caveolin1 upregulation is indirect evidence in addition to the direct data of a decrease in the enzyme activity, that caveolin-1 may play a similar role in AVEC found in the aortic valve similar to the vascular endothelium.

Experiments were performed to determine if Wnt3a secretion changes in the microenvironment of the aortic valve endothelial cells with and without lipids. Figure 4, Panel C, demonstrates that Wnt3a protein concentration in the conditioned media in the presence of LDL with and without Atorvastatin. There is a significant increase in the protein with the lipids and attenuation of this protein secretion with the Atorvastatin treatments. This experiment tests

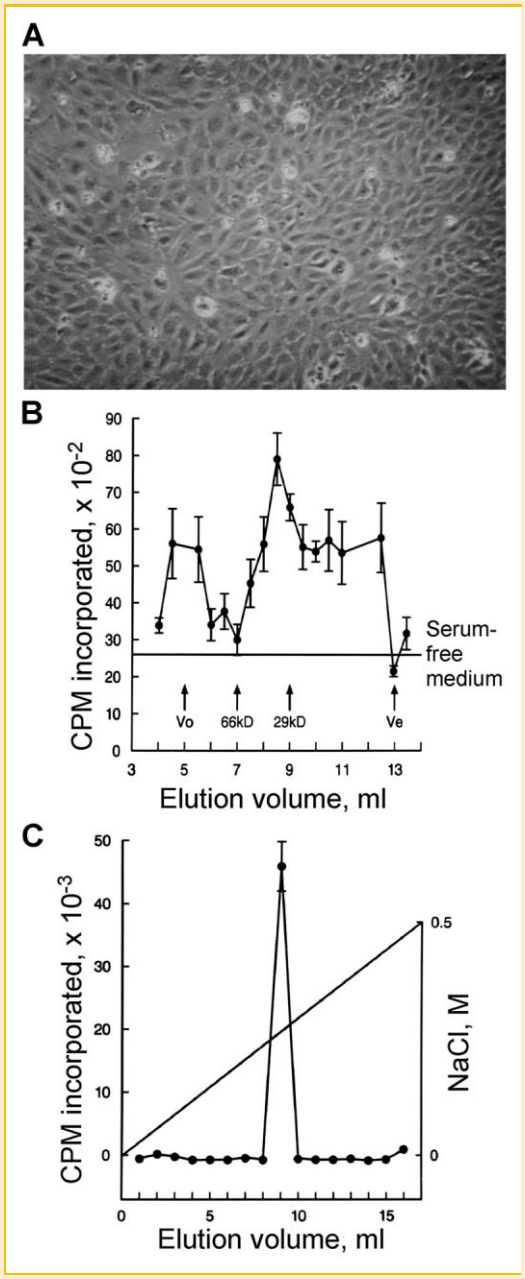

Fig. 3. Protein isolation and characterization of aortic valve endothelial cell conditioned media. Panel (A) light microscopy for aortic valve endothelial cells. Panel (B) cell proliferation for fractions eluting from a DEAE–Sephadex column ($P < 0.001$). Panel (C) fractions from DEAE–Sephadex to characterize weight with Sephadex G-100 ($P < 0.001$).

the effects of lipids regulating the development of a Wnt3a gradient in the microenvironment in parallel with the decreased eNOS functional activity. If LDL increases Wnt3a secretion into the conditioned media or the microenvironment of the diseased aortic valve, this further contributes to the activation of the canonical Wnt pathway in the subendothelial space of the aortic valve. Figure 4, Panel D, demonstrates the Dkk1 expression in the myofibroblast cell after treatment with the conditioned media from the endothelial cells. Dkk1 is the inhibitor of Lrp5 receptor, which is further evidence of the mechanism of Atorvastatin's potential role inhibiting valve calcification via upregulation of Dkk1.

MYOFIBROBLAST CELL DIFFERENTIATING TO OSTEOGENIC BONE

The final experiment tests the myofibroblast cell's ability to differentiate to mineralized bone via upregulation of the Lrp5 receptor. Myofibroblasts were treated with three different conditions to determine the microenvironment necessary to activate the Lrp5 pathway of bone formation. The initial set of conditions includes treatment of the myofibroblasts with osteogenic differentiating media. This osteogenic differentiation media provides the mineralizing microenvironment necessary for the calcification of bone mineralization [Stringa et al., 1995]. The cells were treated with osteogenic media in Figure 5, Panel A, over time the myofibroblast cells stain positive for Alcian blue, indicating the transformation to a chondrocyte phenotype. After 6 weeks, the cells begin to mineralize and form bone as implicated with the positive stain for Alizarin read as shown in Figure 5, Panel B. The microCT indicates mineralization in this in vitro model with upregulation of Runx2 and Lrp5 the key regulators of Wnt regulation of bone formation, Figure 5, Panel C and D.

Next the cells were treated with LDL with and without Atorvastatin directly shown in Figure 5, Panel E. When the cells were treated with lipids directly there was no gene expression of the Lrp5 receptor and low level expression of Runx2 and osteopontin. Figure 5, Panel F, demonstrates the gene expression in myofibroblast cells treated with conditioned media from aortic valve endothelial cells. The conditioned media was produced in the presence of LDL with and without Atorvastatin and in the presence of lipids Wnt3a is secreted into the media. The AEC conditioned media is required to upregulate the Lrp5 gene in this model of endothelial/mesenchymal cross talk. The conditioned media from the endothelial cells treated with lipids induced the Lrp5 gene expression and mildly attenuated with Atorvastatin therapy. Figure 5, Panel G and H, demonstrates the final set of conditions, the response to mechanical force by measuring the Lrp5 expression in the myofibroblast cells with cyclic stress. The Lrp5 is expressed after the application of the cyclic stretch, and is further increased with the application of the cyclic stretch and the Conditioned media treated cells. This data in combination with previously published data [Shao et al., 2005; Rajamannan et al., 2005a; Kirton et al., 2007] indicates that LDL and Pressure are both necessary for the upregulation of the Lrp5/Wnt3a pathway [Rajamannan, 2011bc].

The model proposed in the study as described in Figure 6, provides the cellular architecture for the development of this disease process. The stem cell niche is a unique model for the development of an oxidative stress communication within the aortic valve endothelium. As shown in Figure 6 oxidative stress contributes to the release of Wnt3a into the subendothelial space to activate Lrp5/Frizzled receptor complex on the extracellular membrane of the myofibroblast. This trimeric complex then induces glycogen synthase kinase to be phosphorylated. This phosphorylation event causes β-catenin translocation to the nucleus. β-catenin acts as a coactivator of osteoblast specific transcription factor Runx2 to induce mesenchymal osteoblastogenesis in the aortic valve myofibroblast cell.

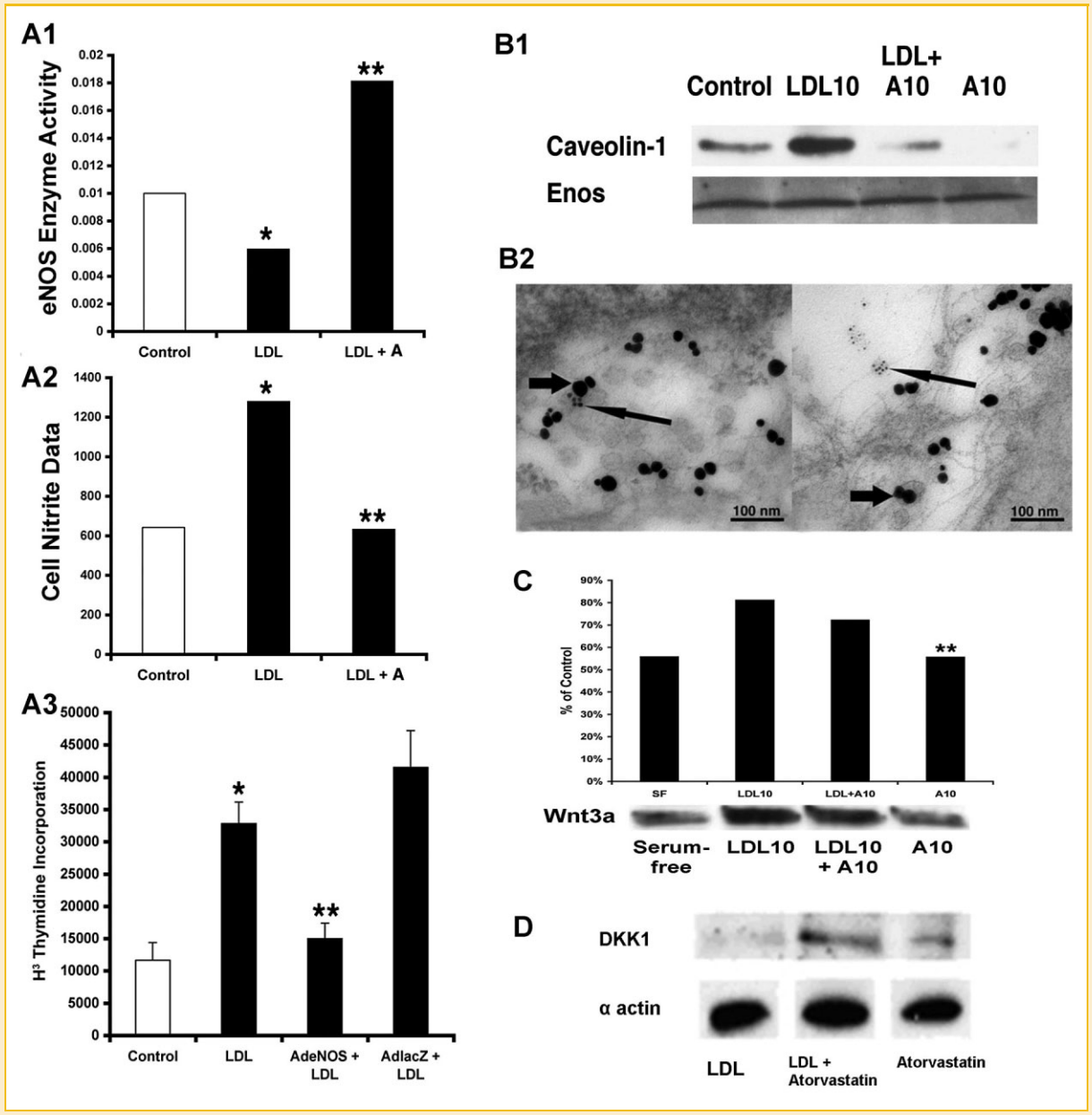

Fig. 4. Evidence for eNOS regulation and Wnt3a secretion from aortic valve endothelial cells. $^{*}P < 0.001$ for control compared to cholesterol, $^{**}P < 0.001$ for cholesterol compared to cholesterol + Atorvastatin. Panel (A) eNOS enzymatic activity, all nitrite data, AdeNOS thymidine data, in the aortic valve endothelial cells (AEC) in the presence of LDL with and without atorvastatin. Panel (B1) Caveolin-1 and eNOS protein expression isolated from the lipid with and without atorvastatin treated cells as shown by Western blot. Panel (B2). Electron microscopy immunogold labeling for eNOS and Caveolin-1 localize in the aortic valve endothelial cells in caveolae. Panel (C) Wnt3a Immunoprecipitate from conditioned media treated with LDL with and without Atorvastatin. Panel (D) Dkk1 protein expression from the myofibroblast cells treated with conditioned media with lipid and with and without atorvastatin treated cells as shown by Western blot.

DISCUSSION

This study demonstrates that in the presence of oxidative stress environment and abnormal mechanical forces the aortic valve develops a mineralizing phenotype via the Lrp5/Wnt3a signaling pathway. For years, CAVD was thought to be due to a degenerative process but recent Working Group by NHLBI, has concluded based on the scientific progress in the field, that the biology is an active process [Rajamannan et al., 2011]. The cell involved in the secretion of Wnt3a is the aortic valve endothelial cell which signals to the adjacent subendothelial cell the myofibroblast cell. The myofibroblast cell is the mesenchymal cell, which has the ability to differentiate to bone, fat, and or cartilage [Liu et al., 2007; Chen et al., 2009]. The results presented in this study demonstrate that a tissue stem cell niche is necessary for the disease mechanism. The physical proximity of the cells, the mechanical pressure and the

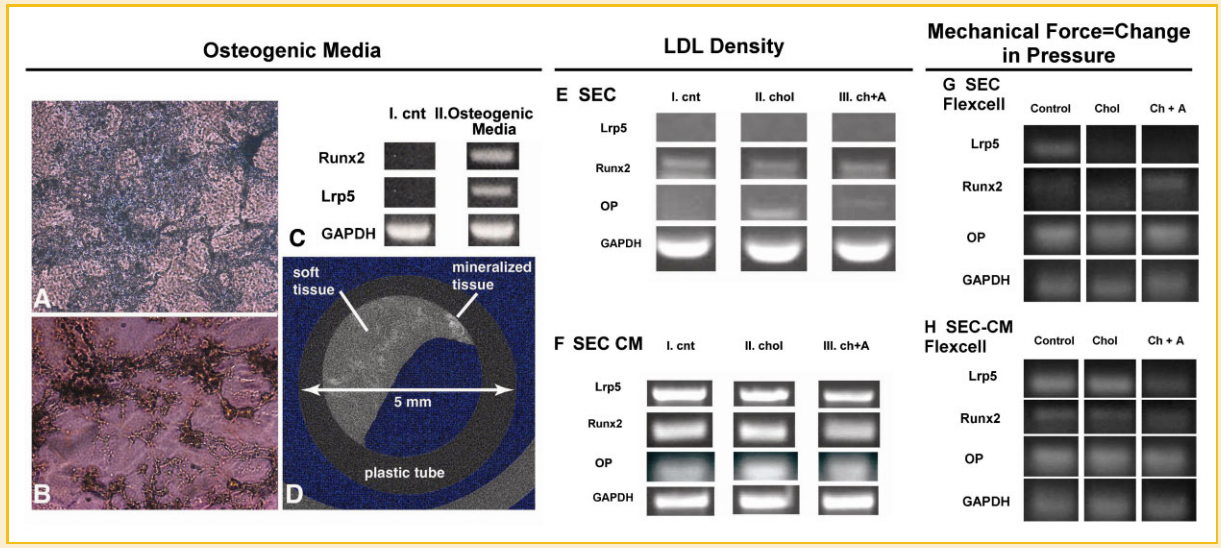

Fig. 5. Osteogenic mineralization assays. Panel (A) the myofibroblast cells stain for Alcian blue, indicating a cartilaginous phenotype treated with osteogenic media. Panel (B) the myofibroblast cells stain positive for Alizarin red, indicating an osteoblast phenotype treated with osteogenic media. Panel (C) RTPCR for Runx2 and Lrp5, in the myofibroblast cells treated with osteogenic media. Panel (D) MicroCT of the calcifying cells indicating mineralization present in the cells. Panel (E) RTPCR for Lrp5, Runx2 and osteopontin in the myofibroblast cells treated with directly with lipids with and without Atorvastatin. Panel (F) RTPCR for Lrp5, Runx2, and osteopontin in the myofibroblast cells treated with conditioned media from Endothelial cells with lipids with and without Atorvastatin. Panel (G) RTPCR for Lrp5, Runx2 and osteopontin in the myofibroblast cells treated with cyclic stretch and with lipids with and without Atorvastatin. Panel (H) RTPCR for Lrp5, Runx2 and osteopontin in the myofibroblast cells treated with cyclic stretch and conditioned media from endothelial cells with lipids with and without Atorvastatin.

hypercholesterolemic environment play a role for the upregulation of the Lrp5 receptor to signal the myofibroblast cell to form bone.

Adult tissues stem cells are a population of functionally undifferentiated cells, capable of (i) homing, (ii) proliferation, (iii) producing differentiated progeny, (iv) self-renewing, (v) regeneration, and (vi) reversibility in the use of these options. Within this definition, stem cells are defined by virtue of their functional potential and not by a specific observable characteristic. This data is the first to implicate a cell–cell communication between the aortic valve endothelial cell and the myofibroblast cell to activate the canonical Wnt pathway. Lrp5/6 is important in normal valve development [Hurlstone et al., 2003; Hassler et al., 2007], in this stem cell niche, reactivation of latent Lrp5 expression [Rajamannan et al., 2005a; Caira et al., 2006; Rajamannan, 2011b], regulates osteoblastogenesis in these mesenchymal cells. The negative bone formation in previously published study hypercholesterolemic $Lrp5^{-/-}$ aortic valves [Rajamannan, 2011b] demonstrate the specificity of the neural crest cardiac derived cells to mineralize via the Lrp5.

The aortic valve endothelial cell communicates with the myofibroblast cell to activate the myofibroblast to differentiate to form an osteoblast-like phenotype [Rajamannan et al., 2003b]. This concept is similar to the endothelial/mesenchymal transition critical in normal valve development [Paruchuri et al., 2006]. This data fulfills these main corollaries of the plausibility of a tissue stem cell niche responsible for the development of valvular heart disease. Within a stem cell niche there is a delicate balance between proliferation and differentiation. Cells near the stem-cell zone are more proliferative, and Wnt likely plays a role in directing cell differentiation. Stem cell behavior is determined by the stem cell's neighboring cell, which in the valve is the endothelial cell. This assumption is aimed at simply describing the fact that cytokines, secreted by cells into the micro-environment are capable of activating quiescent stem cells into differentiation [de Haan et al., 1996].

The main postulate for this corollary stems from the risk factor hypothesis for the development of aortic valve disease and the role of mechanical force mechanism of the Lrp5 receptor. If traditional atherosclerotic risk factors are necessary for the initiation of disease, then these risk factors are responsible for the gradient necessary for the differentiation of myofibroblast cells to become an osteoblast calcifying phenotype [Mohler et al., 1999; Wada et al., 1999; Tintut et al., 2003; Shao et al., 2005; Rajamannan et al., 2005a; Osman et al., 2006; Kirton et al., 2007]. If traditional risk factors are responsible for the development of valvular heart disease, then an oxidative stress mechanism is important for the development of a gradient in this niche. Nitric oxide is important in terms of the mechanism in adult disease processes and also in the developmental abnormalities such as the BAV phenotype in the eNOS null mouse. We have previously published that eNOS is regulated in the aortic valve in an experimental hypercholesterolemia model of valvular disease [Rajamannan et al., 2005b]. A key regulator of eNOS function is caveolin-1 which is expressed in aortic valve endothelial cells [Rajamannan et al., 2002a]. Caveolin-1 upregulation in the presence of lipids inactivates eNOS enzymatic function and further promotes oxidative stress [Garcia-Cardena et al., 1996, 1997].

A well-defined mechanism to inactivate eNOS enzymatic activity is functional binding of eNOS with caveolin1 in the presence of lipids [Blair et al., 1999; Feron et al., 1999]. This data demonstrates that eNOS functional activity is decreased in the aortic valve

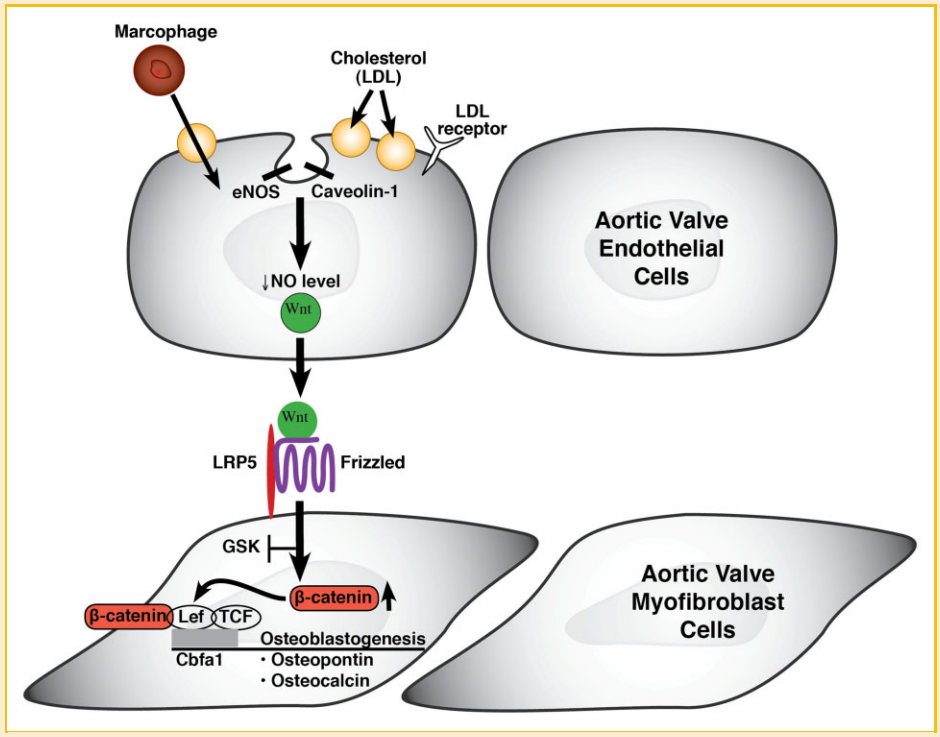

Fig. 6. Schematic modeling for calcification in the aortic valve stem cell niche.

endothelial cells and is regulated similarly to vascular endothelial cells via Caveolin1. Furthermore, in the presence of lipids, Wnt3a is secreted and binds to Lrp5 and Frizzled on the extracellular membrane to regulate the osteoblast gene program. Atorvastatin inhibits the Lrp5 mechanism by an increase in the Dkk1 protein expression in the myofibroblast cells. This developmental disease process follows a parallel signaling pathway that has been observed in the normal embryonic valve development that has been well delineated by previous investigators [Paruchuri et al., 2006]. A similar cell–cell communication is necessary for the development of valve disease. This study provides the correlates described in the mathematical modeling by Agur et al. [2002]. The model of Agur, defines the corollaries necessary to identify a stem cell niche, first the physical architecture of the stem cell niche and second the gradient necessary to regulate the niche. In the BAV the gradient is defined by the niche's microenvironment. The initiation of event of oxidative stress inhibits normal endothelial nitric oxide synthase function, in turn induces Wnt3a secretion to activate bone formation within the valve [Shao et al., 2005; Rajamannan et al., 2005a; Kirton et al., 2007]. This data is the first to implicate a cell–cell communication between the aortic valve endothelial cell and the myofibroblast cell to activate the canonical Wnt pathway. Lrp5 is important in normal valve development [Hurlstone et al., 2003], in this stem cell niche, reactivation of latent Lrp5 expression [Rajamannan et al., 2005a; Caira et al., 2006], regulates osteoblastogenesis in the myofibroblast mesenchymal cells. The two corollary requirements necessary for an adult stem cell niche is to first define the physical architecture of the stem-cell niche and second is to define the gradient of proliferation to differentiation within the stem-cell niche. This concept is similar to the endothelial/mesenchymal transition critical in normal valve development [Paruchuri et al., 2006].

The goal of this study is to determine the two corollaries to define the role of a tissue stem cell niche in CAVD. The corollaries necessary to define a tissue stem cell niche: (1) Physical architecture of the endothelial cells signaling to the adjacent subendothelial cells: the myofibroblast cell. (2) Defining the oxidative-mechanical stress gradient necessary to activate Wnt3a/Lrp5 in this tissue stem cell niche to induce disease. Targeting the Wnt pathway in valvular calcification presents a novel approach towards treating this disease in the future.

ACKNOWLEDGMENTS

This work was completed with the support of 5R01HL085591 and 3R01HL085591S1. Preliminary submission to JCB 9/22/2011. The author is the inventor on a patent for methods to slow progression of valvular heart disease. This patent is owned by the Mayo Clinic and the author does not receive any royalties from this patent.

REFERENCES

Agur Z, Daniel Y, Ginosar Y. 2002. The universal properties of stem cells as pinpointed by a simple discrete model. J Math Biol 44:79–86.

Aikawa E, Nahrendorf M, Sosnovik D, Lok VM, Jaffer FA, Aikawa M, Weissleder R. 2007. Multimodality molecular imaging identifies proteolytic and osteogenic activities in early aortic valve disease. Circulation 115:377–386.

Blair A, Shaul PW, Yuhanna IS, Conrad PA, Smart EJ. 1999. Oxidized low density lipoprotein displaces endothelial nitric-oxide synthase (eNOS) from plasmalemmal caveolae and impairs eNOS activation. J Biol Chem 274: 32512–32519.

Caira FC, Stock SR, Gleason TG, McGee EC, Huang J, Bonow RO, Spelsberg TC, McCarthy PM, Rahimtoola SH, Rajamannan NM. 2006. Human degenerative valve disease is associated with up-regulation of low-density lipoprotein receptor-related protein 5 receptor-mediated bone formation. J Am Coll Cardiol 47:1707–1712.

Chen AF, Jiang SW, Crotty TB, Tsutsui M, Smith LA, O'Brien T, Katusic ZS. 1997. Effects of in vivo adventitial expression of recombinant endothelial nitric oxide synthase gene in cerebral arteries. Proc Natl Acad Sci USA 94: 12568–12573.

Chen JH, Yip CY, Sone ED, Simmons CA. 2009. Identification and characterization of aortic valve mesenchymal progenitor cells with robust osteogenic calcification potential. Am J Pathol 174:1109–1119.

de Haan G, Dontje B, Nijhof W. 1996. Concepts of hemopoietic cell amplification. Synergy, redundancy and pleiotropy of cytokines affecting the regulation of erythropoiesis. Leuk Lymphoma 22:385–394.

Drolet MC, Arsenault M, Couet J. 2003. Experimental aortic valve stenosis in rabbits. J Am Coll Cardiol 41:1211–1217.

Feron O, Dessy C, Moniotte S, Desager JP, Balligand JL. 1999. Hypercholesterolemia decreases nitric oxide production by promoting the interaction of caveolin and endothelial nitric oxide synthase. J Clin Invest 103:897–905.

Garcia-Cardena G, Oh P, Liu J, Schnitzer JE, Sessa WC. 1996. Targeting of nitric oxide synthase to endothelial cell caveolae via palmitoylation: Implications for nitric oxide signaling. Proc Natl Acad Sci USA 93:6448–6453.

Garcia-Cardena G, Martasek P, Masters BS, Skidd PM, Couet J, Li S, Lisanti MP, Sessa WC. 1997. Dissecting the interaction between nitric oxide synthase (NOS) and caveolin. Functional significance of the nos caveolin binding domain in vivo. J Biol Chem 272:25437–25440.

Hassler C, Cruciat CM, Huang YL, Kuriyama S, Mayor R, Niehrs C. 2007. Kremen is required for neural crest induction in *Xenopus* and promotes LRP6-mediated Wnt signaling. Development 134:4255–4263.

Hurlstone AF, Haramis AP, Wienholds E, Begthel H, Korving J, Van Eeden F, Cuppen E, Zivkovic D, Plasterk RH, Clevers H. 2003. The Wnt/beta-catenin pathway regulates cardiac valve formation. Nature 425:633–637.

Kirton JP, Crofts NJ, George SJ, Brennan K, Canfield AE. 2007. Wnt/beta-catenin signaling stimulates chondrogenic and inhibits adipogenic differentiation of pericytes: Potential relevance to vascular disease? Circ Res 101:581–589.

Kovar JL, Simpson MA, Schutz-Geschwender A, Olive DM. 2007. A systematic approach to the development of fluorescent contrast agents for optical imaging of mouse cancer models. Anal Biochem 367: 1–12.

Lee TC, Zhao YD, Courtman DW, Stewart DJ. 2000. Abnormal aortic valve development in mice lacking endothelial nitric oxide synthase. Circulation 101:2345–2348.

Liu AC, Joag VR, Gotlieb AI. 2007. The emerging role of valve interstitial cell phenotypes in regulating heart valve pathobiology. Am J Pathol 171:1407–1418.

Makkena B, Salti H, Subramaniam M, Thennapan S, Bonow RH, Caira F, Bonow RO, Spelsberg TC, Rajamannan NM. 2005. Atorvastatin decreases cellular proliferation and bone matrix expression in the hypercholesterolemic mitral valve. J Am Coll Cardiol 45:631–633.

Mohler ER 3rd, Chawla MK, Chang AW, Vyavahare N, Levy RJ, Graham L, Gannon FH. 1999. Identification and characterization of calcifying valve cells from human and canine aortic valves. J Heart Valve Dis 8:254–260.

Mohler ER 3rd, Gannon F, Reynolds C, Zimmerman R, Keane MG, Kaplan FS. 2001. Bone formation and inflammation in cardiac valves. Circulation 103:1522–1528.

Osman L, Yacoub MH, Latif N, Amrani M, Chester AH. 2006. Role of human valve interstitial cells in valve calcification and their response to atorvastatin. Circulation 114:I547–I552.

Paruchuri S, Yang JH, Aikawa E, Melero-Martin JM, Khan ZA, Loukogeorgakis S, Schoen FJ, Bischoff J. 2006. Human pulmonary valve progenitor cells exhibit endothelial/mesenchymal plasticity in response to vascular endothelial growth factor-A and transforming growth factor-beta2. Circ Res 99:861–869.

Rajamannan NM. 2011a. Bicuspid aortic valve disease: The role of oxidative stress in Lrp5 bone formation. Cardiovasc Pathol 3:168–176.

Rajamannan NM. 2011b. The role of Lrp5/6 in cardiac valve disease: Experimental hypercholesterolemia in the ApoE$^{-/-}$/Lrp5$^{-/-}$ mice. J Cell Biochem 112:2987–2991.

Rajamannan NM. 2011c. The Role of Lrp5/6 in cardiac valve disease: LDL-density-pressure theory. J Cell Biochem 112:2222–2229.

Rajamannan NM, Helgeson SC, Johnson CM. 1988. Anionic growth factor activity from cardiac valve endothelial cells: Partial purification and characterization. Clin Res 36:309A.

Rajamannan NM, Caplice N, Anthikad F, Sebo TJ, Orszulak TA, Edwards WD, Tajik J, Schwartz RS. 2001a. Cell proliferation in carcinoid valve disease: A mechanism for serotonin effects. J Heart Valve Dis 10:827–831.

Rajamannan NM, Sangiorgi G, Springett M, Arnold K, Mohacsi T, Spagnoli LG, Edwards WD, Tajik AJ, Schwartz RS. 2001b. Experimental hypercholesterolemia induces apoptosis in the aortic valve. J Heart Valve Dis 10:371–374.

Rajamannan NM, Springett MJ, Pederson LG, Carmichael SW. 2002a. Localization of caveolin 1 in aortic valve endothelial cells using antigen retrieval. J Histochem Cytochem 50:617–628.

Rajamannan NM, Subramaniam M, Springett M, Sebo TC, Niekrasz M, McConnell JP, Singh RJ, Stone NJ, Bonow RO, Spelsberg TC. 2002b. Atorvastatin inhibits hypercholesterolemia-induced cellular proliferation and bone matrix production in the rabbit aortic valve. Circulation 105:2260–2265.

Rajamannan NM, Edwards WD, Spelsberg TC. 2003a. Hypercholesterolemic aortic-valve disease. N Engl J Med 349:717–718.

Rajamannan NM, Subramaniam M, Rickard D, Stock SR, Donovan J, Springett M, Orszulak T, Fullerton DA, Tajik AJ, Bonow RO, Spelsberg T. 2003b. Human aortic valve calcification is associated with an osteoblast phenotype. Circulation 107:2181–2184.

Rajamannan NM, Subramaniam M, Caira F, Stock SR, Spelsberg TC. 2005a. Atorvastatin inhibits hypercholesterolemia-induced calcification in the aortic valves via the Lrp5 receptor pathway. Circulation 112:I229–I234.

Rajamannan NM, Subramaniam M, Stock SR, Stone NJ, Springett M, Ignatiev KI, McConnell JP, Singh RJ, Bonow RO, Spelsberg TC. 2005b. Atorvastatin inhibits calcification and enhances nitric oxide synthase production in the hypercholesterolaemic aortic valve. Heart 91:806–810.

Rajamannan NM, Evans FJ, Aikawa E, Grande-Allen KJ, Demer LL, Heistad DD, Simmons CA, Masters KS, Mathieu P, O'Brien KD, Schoen FJ, Towler DA, Yoganathan AP, Otto CM. 2011. Calcific aortic valve disease: Not simply a degenerative process: A review and agenda for research from the National Heart and Lung and Blood Institute Aortic Stenosis Working Group. Executive summary: Calcific aortic valve disease-2011 update. Circulation 124: 1783–1791.

Roberts WC, Ko JM. 2005. Frequency by decades of unicuspid, bicuspid, and tricuspid aortic valves in adults having isolated aortic valve replacement for aortic stenosis, with or without associated aortic regurgitation. Circulation 111:920–925.

Shah V, Haddad FG, Garcia-Cardena G, Frangos JA, Mennone A, Groszmann RJ, Sessa WC. 1997. Liver sinusoidal endothelial cells are responsible for

nitric oxide modulation of resistance in the hepatic sinusoids. J Clin Invest 100:2923–2930.

Shah V, Toruner M, Haddad F, Cadelina G, Papapetropoulos A, Choo K, Sessa WC, Groszmann RJ. 1999. Impaired endothelial nitric oxide synthase activity associated with enhanced caveolin binding in experimental cirrhosis in the rat. Gastroenterology 117:1222–1228.

Shao JS, Cheng SL, Pingsterhaus JM, Charlton-Kachigian N, Loewy AP, Towler DA. 2005. Msx2 promotes cardiovascular calcification by activating paracrine Wnt signals. J Clin Invest 115:1210–1220.

Stringa E, Filanti C, Giunciuglio D, Albini A, Manduca P. 1995. Osteoblastic cells from rat long bone. I. Characterization of their differentiation in culture. Bone 16:663–670.

Tintut Y, Alfonso Z, Saini T, Radcliff K, Watson K, Bostrom K, Demer LL. 2003. Multilineage potential of cells from the artery wall. Circulation 108:2505–2510.

Wada T, McKee MD, Steitz S, Giachelli CM. 1999. Calcification of vascular smooth muscle cell cultures: Inhibition by osteopontin. Circ Res 84:166–178.

Weiss RM, Ohashi M, Miller JD, Young SG, Heistad DD. 2006. Calcific aortic valve stenosis in old hypercholesterolemic mice. Circulation 114: 2065–2069.

Westerlind KC, Wronski TJ, Ritman EL, Luo ZP, An KN, Bell NH, Turner RT, Turner RT. 1997. Estrogen regulates the rate of bone turnover but bone balance in ovariectomized rats is modulated by prevailing mechanical strain. Proc Natl Acad Sci USA 94:4199–4204.